JET–R(00)04

V I Afanasyev
A Gondhalekar
A I Kislyakov

On the Possibility of Determining the Radial Profile of Hydrogen Isotope Composition of JET Plasmas, and of Deducing Radial Transport of the Isotope Ions

JET–R(00)04

On the Possibility of Determining the Radial Profile of Hydrogen Isotope Composition of JET Plasmas, and of Deducing Radial Transport of the Isotope Ions

V I Afanasyev[1], A Gondhalekar, A I Kislyakov[1].

JET Joint Undertaking, Abingdon, Oxfordshire, OX14 3EA,
[1]A F Ioffe Physico-Technical Institute, St. Petersburg, Russia.

October 2000

ABSTRACT

Measurements of internal hydrogen isotopic composition of plasmas in JET and elsewhere have been lacking. In this report we show that it is feasible to determine the profile of relative hydrogen isotope density, using a neutral particle analyzer. Using detailed modeling of the formation of atomic flux and its measurement, we have quantified sensitivity of the deduced plasma composition to uncertainty of plasma parameters that impact on the measurement. We have tested application of the proposed methodology by experimentally determining the perturbed deuteron density profile in a hydrogen plasma, when the deuteron density at the plasma edge was modulated using a short pulse of deuterium gas. We have also determined the deuteron density diffusivity. The determinations are very crude at present; however this exercise is intended to enable us to design better experiments to determine plasma isotopic composition and the radial isotope ion diffusivities.

1. INTRODUCTION.

An important measurement deficiency during the deuterium-tritium fusion experiments in JET and TFTR has been the absence of experimental determination of the isotopic composition of the plasma in the central region. This gave rise to uncertainty in (a) energy transport analysis due to the possibility of ion mass dependence of local thermal transport coefficients, (b) the analysis of α-particle heating of electrons due to the possibility of an isotope effect on energy transport as mentioned above, and uncertainty in equilibration power to the electrons from hotter plasma fuel ions, (c) analysis of ICRF heating of plasmas with multiple hydrogen isotope ions in simultaneous resonance, where the wave dispersion and power sharing between different ions depend on the isotope density. Crucially, predictions of hydrogen isotope ion density in future larger tokamak fusion plasmas are not reliable. Knowledge of particle transport in tokamak plasmas is flimsy and a reliable relationship between sources and an equilibrium ion density profile can not be established with confidence. Thus, measurement of hydrogen isotope ion transport is another key requirement.

In this report we propose to investigate the questions: (a) is it feasible in JET plasmas, using a neutral particle analyzer (NPA), to determine the radial profile of relative hydrogen isotope ion density? and (b) is it then possible to determine radial diffusivities of hydrogen isotope ions by modulation of the density at the plasma edge by gas injection and measuring evolution of the perturbed density profile? Following factors facilitate such a measurement:

1. The NPA makes simultaneous measurements of energy distribution of efflux of atoms of different hydrogen isotopes (H, D and T) from the plasma. The atomic flux, produced by charge-exchange (CX) reactions between plasma ions and thermal hydrogen isotope atoms in the plasma, is proportional to hydrogen isotope ion and atom densities. The rate of production of CX atoms is given by $n_i n_A < \sigma\upsilon >$, where $n_i(r,t)$ is the isotope ion density, $n_A(r,t)$ is the density of hydrogenic atoms, and $< \sigma\upsilon >$ is an appropriately averaged rate-coefficient for CX.

2. Corresponding to every energy of the exiting atoms is a spatial emissivity profile, which gives the location of the source of the measured flux.
3. On the way out of the plasma the atomic flux is attenuated, due to reionization by CX and collisions. Coefficients for attenuation depend only on the speed of the exiting hydrogenic atoms, and therefore relative isotope fluxes are reliably scaleable.
4. Normally, the largest contribution to fueling of the plasma is recycling at the plasma edge. Therefore injecting additional gas at the edge does not greatly perturb the normal evolution of radial ion density profiles. Moreover, the perturbed radial atom density profile reaches steady-state in a much shorter time than the perturbed ion density profile, and therefore evolution of the atomic and ion species can be treated independently.

Therefore, measurement of energy dependence of ratio of isotope atom fluxes would enable us to deduce radial profile of the isotope ion density ratio in the plasma. Using independent measurements of profile of total ion density, profiles of the isotope ion densities may be determined. Analysis of temporal behavior of these profiles after modulating the source of one isotope by gas injection at the plasma edge would enable us to determine diffusion of the modulated ion species into the plasma.

In order to determine the feasibility of using the above method in JET plasmas, and to estimate its limitations, we need to (i) simulate formation of the hydrogen isotope atomic fluxes to obtain a relation between energy of atoms and radial location from which they are emitted, (ii) determine sensitivity of the measured isotope flux ratio to uncertainties in the key plasma parameters which control production and transmission of flux of atoms. In section 2 we describe a model for atomic transport in plasmas and formation of the atomic efflux. In section 3 the uncertainty in the flux ratio due to uncertainty in other key plasma parameters is investigated. In section 4 we analyze measurements in which the procedure outlined above was applied with the aim to determine deuteron density diffusivity in a hydrogen plasma.

2. FORMULATION OF KINETIC EQUATION FOR COMPUTATION OF RADIAL DENSITY PROFILE OF THERMAL HYDROGENIC ATOMS IN THE PLASMA DUE TO RECYCLING AT THE PLASMA EDGE.

To simulate CX of hydrogen isotope ions (protons, deuterons and tritons) in the plasma and efflux of resulting atoms we need to calculate the radial profile of density of thermal hydrogenic atoms in the plasma, whose source is the first wall. To this end we apply a model developed by Dnestrovskij[1], which is based on solution of a kinetic equation for transport of atoms in a plasma. It has been shown [1] that when the plasma is optically thick to the atoms, i.e. $\bar{n}\sigma_{cx}a >> 1$, (where $\bar{n}$ is the average plasma electron and ion density, $\sigma_{cx} \cong 2\times10^{-19} m^{-2}$, is the CX cross-section, and a is the linear dimension of the plasma), then the velocity distribution of the atoms

is well described by a kinetic equation. JET plasmas, typically with $a \approx 1m$ and $\bar{n} \geq 3\times10^{19} m^{-3}$, satisfy the requirement. It was shown in ref. [2] that a one-dimensional slab model adequately describes transport of atoms in the plasma in tokamak geometry. For an infinite slab plasma, bounded by the first wall on two sides at $-a \leq x \leq a$, the equation for velocity distribution of the atoms is written as

$$\upsilon \frac{\partial f}{\partial x} + Sf = (S_{cx}N + S_r n_e)\varphi_i \tag{1}$$

Here, $f(x,\upsilon)$ and $\varphi_i(x,\upsilon)$ are respectively the velocity distributions for the atoms and plasma ions, and $S(\upsilon) = S_{cx}(\upsilon) + S_e(\upsilon) + S_i(\upsilon)$,

Where $S_{cx} = <\sigma_{cx}\upsilon_0> n_i$, $S_i = \langle\sigma_i \upsilon_i\rangle n_i$, $S_e = \langle\sigma_e\upsilon_e\rangle n_e$, and $S_r = \langle\sigma_r\upsilon_e\rangle n_e$. (2)

S_{cx}, S_i, S_e, and S_r are respectively rate coefficients for CX, ionization by ion impact and electron impact, and radiative recombination; and σ are corresponding cross-sections. $N(x)$, $n_i(x)$, and $n_e(x)$ are respectively densities of the atoms, plasma ions and electrons. Moreover, $n_i(x) = n_e(x) = n(x)$. υ_0, υ_i, υ_e are thermal velocities of the atoms, plasma ions and electrons. Brackets $\langle\rangle$ signify average over assumed Maxwellian velocity distributions of the two reacting species, defined as

$$\langle\sigma\upsilon\rangle = \int f_1(x,\upsilon_1) f_2(x,\upsilon_2) \mid \upsilon_1 - \upsilon_2 \mid \sigma(\mid \upsilon_1 - \upsilon_2 \mid) d\upsilon_1 d\upsilon_2$$

Because usually $\upsilon_e >> \upsilon_0$ and υ_i, then processes involving collisions with electrons can be simplified as

$$\langle\sigma_e\upsilon_e\rangle = \int \varphi_e(x,\upsilon_e')\sigma_e(\upsilon_e')\upsilon_e' d\upsilon_e',$$

and $$\langle\sigma_r\upsilon_e\rangle = \int \varphi_e(x,\upsilon_e')\sigma_r(\upsilon_e')\upsilon_e' d\upsilon_e'. \tag{3}$$

Processes involving collisions with ions are also simplified for convenience, owing to weak variation of σ_{cx} and σ_i in a given small energy interval of interest,

$$\langle\sigma_{cx}\upsilon_i\rangle = \int \varphi_i(x,\upsilon_i')\sigma_{cx}(\upsilon_i')\upsilon_i' d\upsilon_i',$$

and $$\langle\sigma_i\upsilon_i\rangle = \int \varphi_i(x,\upsilon_i')\sigma_i(\upsilon_i')\upsilon_i' d\upsilon_i'. \tag{4}$$

The density and velocity of the atoms in the plasma at the boundary at $x = \pm a$ are taken as $N(\pm a) = N_0$ and $\upsilon(\pm a) = V_0$ respectively. The spatial distribution of number density of atoms in the plasma, which is connected with their velocity distribution function through a relation $N(x) = \int_{-\infty}^{\infty} f(x,\upsilon) d\upsilon$, is then obtained from Eq. (1) in integral form[1],

$$N(x) = N^0(x) + \int_{-a}^{a} n(\xi)K(x,\xi)N(\xi)d\xi + \int_{-a}^{a} n^2(\xi)R(x,\xi)d\xi \tag{5}$$

Here
$$N^0(x) = N_0 \times \cosh\left(\frac{1}{\upsilon_0}\int_0^x S dx'\right) \Big/ \cosh\left(\frac{1}{\upsilon_0}\int_0^a S dx'\right) \tag{6}$$

and
$$K(x,\xi) = \int_0^\infty d\upsilon \frac{\langle \sigma_{cx}\upsilon_i \rangle}{\upsilon_i}\varphi_i \, exp\left(-sinh(x-\xi)\int_\xi^x \frac{S}{\upsilon}dx'\right) \tag{7}$$

and
$$R(x,\xi) = \langle \sigma_r \upsilon_e \rangle \int_0^\infty d\upsilon \frac{\varphi_i}{\upsilon} exp\left(-sinh(x-\xi)\int_\xi^x \frac{S}{\upsilon}dx'\right) \tag{8}$$

In the absence of neutral beam injection (NBI), the density of hydrogenic atoms at a point (x) in the plasma is due to two sources: (i) cool "primary" atoms entering the plasma through its boundary and reaching the layer at (x) without charge-exchange, but with attenuated density due to losses during transit through the plasma, as given by eq.(6), (ii) hot "secondary" atoms from elsewhere in the plasma formed due to multiple charge-exchange of "primary" atoms and due to radiative recombination. Although the recombination cross-section is very small, in the large dimensioned, dense, and hot thermonuclear plasmas it may become significant [3].

Equation (5) can be solved using the method of successive approximations[1]. Finally the velocity distribution of the flux of atoms emitted by plasma is given by

$$\Gamma(\upsilon) = \upsilon f(\upsilon) = \int_{-a}^{a} dx\left(S_{cx}N + S_r n_e\right)\varphi_i(x,\upsilon)\left(\frac{1}{\upsilon}\int_a^x S(x',\upsilon)dx'\right) \tag{9}$$

Here $f(\upsilon)$ and $\varphi_i(x,\upsilon)$ are as defined earlier, and $\Gamma(\upsilon)$ is atomic flux per unit plasma surface area and per unit solid angle, directed perpendicular to the plasma surface. An emissivity function for the atomic flux, defined as $\varepsilon(x,\upsilon)=d\Gamma(x,\upsilon)/dx$, gives the spatial distribution of location in the plasma from which the measured atomic flux of a given energy originates.

The approach described was implemented in a numerical code developed by Izvozchikov[4]. The code has been generalized to the case of multi-component plasma, making it suitable for investigations of plasma with a mixture of ionic species, H, D, T, and He, all with different radial density distributions. The atomic flux, its energy distribution, and the emissivity function of each plasma component can be simulated for the "passive" case (i.e. without NBI), and "active" case (with externally injected beam of atoms as targets for CX with plasma ions). The code was used to model efflux of atoms from JET plasmas and test its sensitivity to uncertainty of the controlling plasma parameters. In section 3 we analyze only the "passive" case, corresponding to the NPA measurements to be subsequently analyzed in section 4.

3. SIMULATIONS TO TEST THE SENSITIVITY OF MEASURED RATIO OF ATOMIC HYDROGEN ISOTOPE FLUXES TO UNCERTAINTIES IN THE PLASMA PARAMETERS CONTROLLING THE FLUX.

In Section 4 we shall analyze measurements from an experiment in which a deuterium gas pulse was injected into a hydrogen plasma. Therefore we simulate formation of atomic fluxes in a hydrogen-deuterium plasma to test the sensitivities. Results of the simulation can easily be generalized to other combinations of H/D/T for plasma and gas pulse species. We consider only plasmas with Maxwellian electron and ion energy distributions, such as for Ohmic heated (OH) plasmas. Table I gives representative assumed radial profiles of electron and ion density, and corresponding temperatures used in the simulation. Assumed hydrogen isotope atom densities and temperatures at the plasma edge are also given.

Table I: Reference plasma parameters

Minor radius $a[m] = 1.0$

$$n_e(r)[m^{-3}] = 3.1\times10^{19}\times[1-(r/a)^6]$$

$$n_{H+}(r)[m^{-3}] = 2.7\times10^{19}\times[1-(r/a)^6]$$

$$T_e(r)[keV] = 3.1\times[1-(r/a)^{1.2}]^{0.9} + T_e(a)$$

$$T_i(r)[keV] = T_{i0}\times[1-(r/a)^2] + T_i(a)$$

where

Peak ion temperature	$T_{i0} = 2$
Edge ion and electron temperatures	$T_i(a) = 0.05$ and $T_e(a) = 0.05$
Isotope ion density ratio	$n_{D+}(r)/n_{H+}(r) = 0.1$
Edge isotope atom density ratio	$n_{D0}(a)/n_{H0}(a) = 0.1$
Total atom density at edge	$n_{H0}(a) + n_{D0}(a) = 1.1\times10^{16}m^{-3}$
Edge isotope atom temperatures	$T_{D0}(a) = T_{H0}(a) = 10eV$
Main plasma impurity is carbon, giving	$Z_{eff} = 1.3$

Fig.1 shows the profiles. Eq.5 was used to compute radial profiles of density of hydrogen and deuterium atoms for the reference plasma, and the results are shown in fig.2. The density of atoms at the plasma edge is usually not measured, it is a free parameter whose magnitude can be deduced by iteration to obtain agreement of calculated flux and measured absolute fluxes to the NPA, $\Gamma_{H0}(E)$ and $\Gamma_{D0}(E)$. In the example shown in fig.2 total density of atoms at the plasma edge was chosen to be $1.1\times10^{16}m^{-3}$. For the reference plasma, the spatial emissivity function of atoms reaching the NPA, defined as integrand of eq.9, was calculated for different energies of

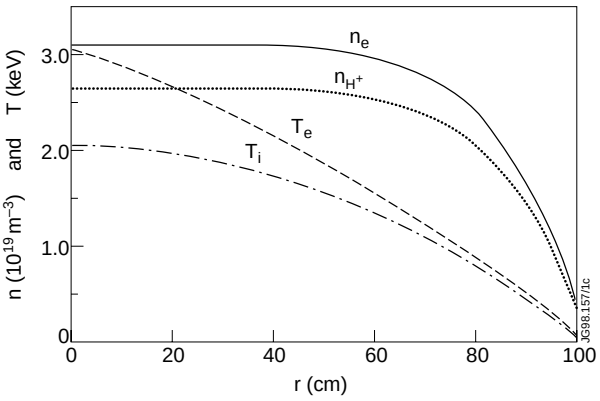

Fig.1: Radial profiles of main pertinent parameters for the reference OH plasma as given in Table 1. Ratio of radial isotope ion densities is specified to be constant, $R_n(r) = n_{D+}(r) / n_{H+}(r) = 0.1$.

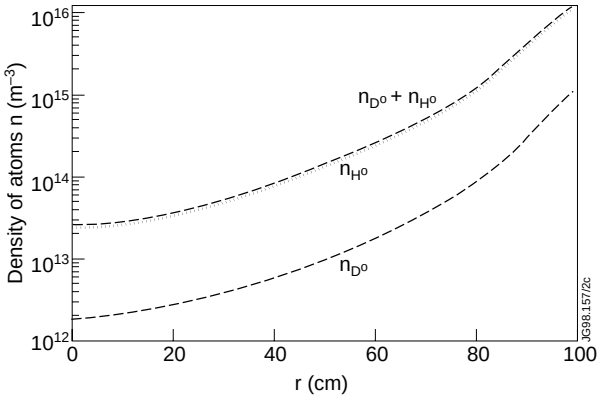

Fig.2: Radial distribution of density of hydrogen and deuterium atoms, $n_{H0}(r)$ *and* $n_{D0}(r)$*, calculated using eq.5 as implemented in the code DOUBLE.*

atoms. Fig.3 shows normalized radial emissivity functions for D and H atoms of four different energies, the normalization factor for the four pairs of curves is also given. Notice that to measure even this small energy range a detection system with a dynamic range of more than six orders of magnitude is required. We see that the emissivity functions for atoms of different hydrogen isotopes of equal energy are spatially close to each other. For H and D atoms in the energy range 2-20 keV the maxima in emission are located in the core region 35≤ r(cm) ≤85. In order to probe the plasma closer to the core atoms of higher energy have to be measured. However we discuss here only the energy range 2-20keV because at the low ion temperature in the plasmas considered the ratio of fluxes to the NPA at the highest and lowest energies is $\sim 10^6$, at the limit of meaningful counting rates in the NPA used. Spatial resolution of the location of the emission, defined as width at half height of the emissivity function, is found to be 16-52 cm. We therefore define uncertainty in location of the source of measured atoms as ±8 ≤Δr(cm)≤ ±26. The fifteen channels of the NPA can span energies 2≤E(keV)≤200, which could be used to access deeper regions of the plasma. In order to receive sufficient flux into the NPA at energies corresponding to the core of the plasma the ion temperature needs to be higher than that in this reference case. Plasmas such as in the hot-ion H-mode in JET would be more suitable for deeper probing.

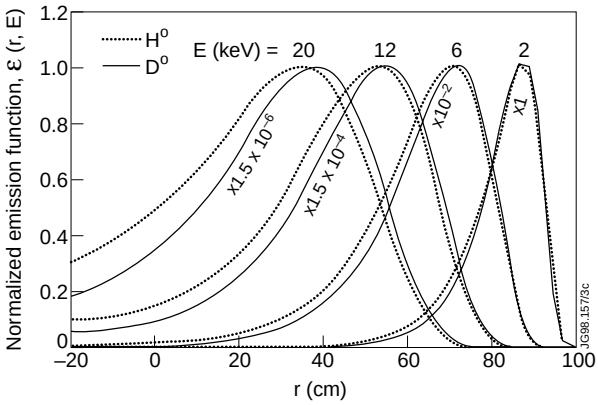

Fig.3: Radial variation of emissivity functions, $\varepsilon_{D0}(r,E)$ *and* $\varepsilon_{H0}(r,E)$*, for deuterium and hydrogen atoms measured outside the plasma. Functions* $\varepsilon(r,E)$ *give the relative probability that the atoms of energy E detected outside the plasma originated at the location r(cm) in the plasma.*

3.1. Variation with energy of isotope flux ratio on radial variation of hydrogen isotope ion density ratio.

Since all pertinent rate coefficients in these considerations depend on the speed of atoms, the atomic flux ratio shall be normalized thus $R_\Gamma(E) = [\Gamma_{D0}(E)/\Gamma_{H0}(E)] \times [m_D/m_H]^{1/2}$. Since the atomic flux of energy E is associated with a radial position, we can transform $R_\Gamma(E) \rightarrow R_\Gamma(r)$. In order to test dependence of radial profile of the normalized isotope atom flux ratio $R_\Gamma(r)$ on radial profile of isotope ion density ratio $R_n(r) = n_{D+}(r)/n_{H+}(r)$ we have simulated a plasma with parameters of the reference case using $R_n(r) = 0.1 + 0.8(r/a)^2$. We have assumed that the isotope ion temperatures are equal everywhere, $T_{D+}(r) = T_{H+}(r)$. Results of the simulation are shown in fig.4 for fluxes at energies E(keV) = 2, 6, 12 and 20. As shown in fig.3, the maxima in emissivity functions corresponding to these energies are centered at radii r(cm) = 84, 68, 48 and 26. In fig.4 the diffuse spatial origin of the flux is shown as horizontal bars, which give the full width at half maximum of the emissivity function. In fig.5 a comparison is shown of $R_\Gamma(r)$ for two different profiles of isotope ion density ratio, $R_n(r) = 0.1 + 0.8 \cdot (r/a)^2$ and $R_n(r) = 0.1$. The deviations of $R_\Gamma(r)$ from $R_n(r)$ are due to speed dependent transmission coefficient for the two isotope atoms, the transmission of deuterium atoms is smaller than for hydrogen atoms, due to lower speed. Agreement is found between $R_n(r)$ and $R_\Gamma(r)$, which is encouraging for our objective of determining the relative isotope density profile by measuring relative isotope fluxes at different energies.

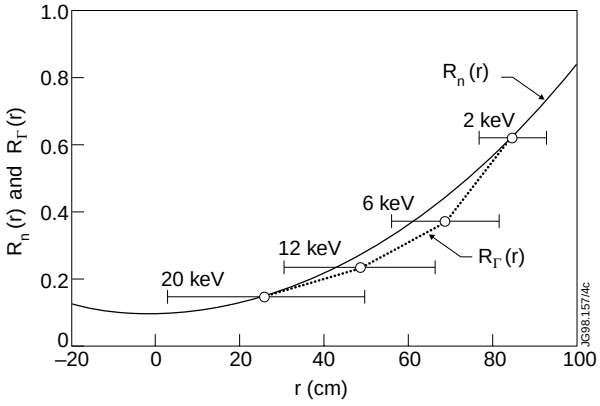

Fig.4: Variation of the ratio of emissivity functions $R_\varepsilon(r) = \varepsilon_{D0}(r)/\varepsilon_{H0}(r)$ for specified radial isotope density ratio, $R_n(r) = 0.1 + 0.8(r/a)^2$.

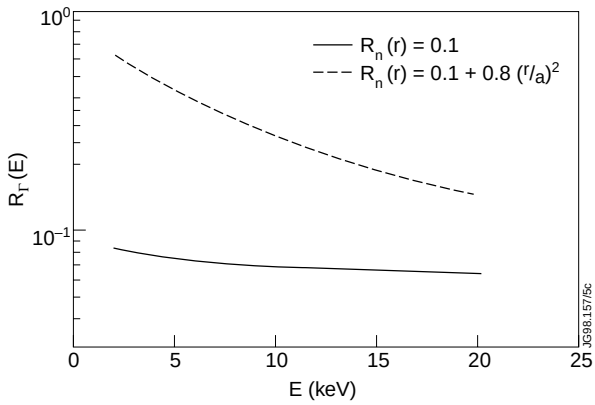

Fig.5: Dependence of ratio of normalized flux $R_\Gamma(E)$ on E, for two radial profiles of ratio of isotope ion densities, $R_n(r)$.

3.2. Sensitivity of isotope flux ratio to differences in isotope ion temperatures.

However, the measured ratio $R_\Gamma(E)$ is sensitive not only to the isotope ion density ratio $R_n(r)$ but also very strongly dependent on the isotope ion temperature ratio $R_T(r) = T_{D+}(r)/T_{H+}(r)$. This is because of the exponential dependence of ion population on ion energy in Maxwellian plasmas. In determining $R_\Gamma(E)$ in section 3.1 we have assumed that ions of the two isotopes

have exactly equal temperatures everywhere along the line-of-sight. We can not be certain that this assumption is applicable. We have therefore tested the effect of uncertainty in isotope ion temperatures, by allowing the isotope ion temperatures to deviate from equality, uniformly along the line-of-sight. Keeping $R_n(r)=0.1$ we have varied $[T_{D+}(r)-T_{H+}(r)]/T_{H+}(r)$ by adjusting $T_{D+}(0)$ and computing $R_\Gamma(E)$. Fig.6 shows the result, that even small differences in temperatures of the two isotope ions can give rise to large variation in the measured $R_\Gamma(E)$, for example a 5% difference in temperature will change $R_\Gamma(E)$ at 20keV by a factor ~1.6 compared to that for $R_T(r)=1$. Thus large uncertainty in the inferred isotope density ratio will arise simply because of uncertainty in isotope ion temperatures.

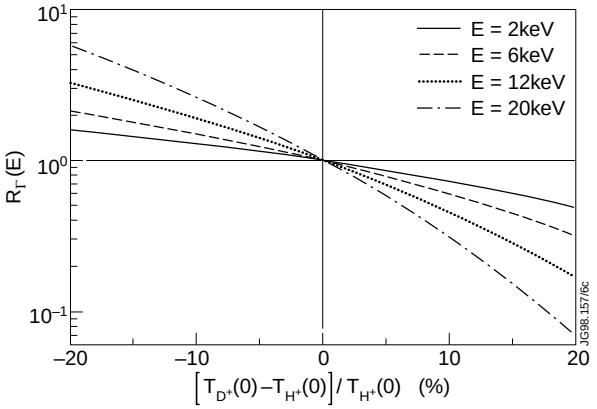

Fig.6: Deviation of isotope flux ratio $R_\Gamma(E)$ from unity due to variation in isotope ion temperatures. $R_\Gamma(E)$ for four energies, E(keV) = 2, 6, 12, 20, is shown. Corresponding centers of hydrogen emissivity function are located at r(cm) = 84, 68, 48, and 26. The hydrogen ion temperatures at positions of these centers are T_{H+}(keV)=0.7, 1.3, 1.7, 1.9 respectively.

Can this uncertainty be ameliorated by using self-consistent "effective" ion temperatures $T_H^{eff}(E)$ and $T_D^{eff}(E)$, deduced from the measured fluxes? "Effective" temperature is defined

$$T^{eff}(E)=-1\Big/\left(\frac{d}{dE}\left(ln\frac{\Gamma(E)}{\sqrt{E}}\right)\right)$$

From fig.5 we see that even with $R_n(r)$=constant, measured $R_\Gamma(E)$ is larger at low energies compared to that at higher energies, due to different attenuation and emissivity profiles for the two isotope fluxes. This has the consequence that even for $R_T(r)=1$ the $T^{eff}(E)$ for the two isotope ions will be different. We have computed $T^{eff}(E)$ for both species of atoms at different energies E, with $R_n(r)=0.1$, and $R_T(r)=1$. The result is displayed in fig.7 in the form $[T_D^{eff}(E)-T_H^{eff}(E)]/T_H^{eff}(E=2keV)$ Vs E.

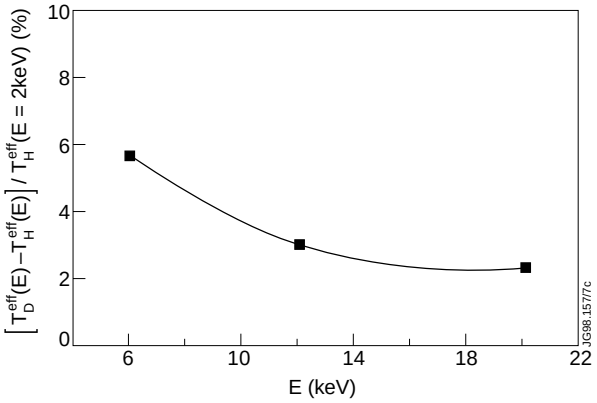

Fig.7: Apparent differences in $T^{eff}(E)$ for the deuterium and hydrogen ions, arising entirely due to differences in plasma transparancy and location of emissivity functions of the two isotopes.

We see that an apparent difference, ranging from 2% at $E=20keV$ to 6% at $E=6keV$, emerges in the temperatures of the two isotopes deduced from measurements of the fluxes in the energy range 2-20 keV. Referring to fig.6 this 2-6% uncertainty in isotope temperatures translates into up to 20-40% uncertainty in isotope flux ratio.

3.3. Sensitivity of position of peak of emissivity to peakedness of isotope ion temperature profile $T_i(r)$.

The shape of the isotope ion temperature profile will determine the location of the emissivity function ε(r,E) for atoms. To determine the magnitude of the radial shift in ε(r,E) due to different ion temperature profiles we have modeled ε(r,E) for different peakedness of $T_i(r)$, assuming that $T_i(r)$ for both isotopes are identical. Fig.8 shows four ion temperature profiles with different peakedness index α, $T_i(r) = T_i(0)\left(1-(r/a)^2\right)^{\alpha}$, $\alpha = 1$ corresponds to the reference case. Simulations of ε(r,E) were made for different energies, as in fig.3, and the spatial location of the peak of ε(r,E) was found to move according to peakedness of $T_i(r)$. Taking as reference the ion temperature at the position of peak in ε(r,E) for $\alpha = 1$, then Δr_{Ti} is the radial shift in position of the point with the same ion temperature; this definition of Δr_{Ti} is illustrated in fig.8. Next, the shift in position of the peak in emissivity is shown as Δr_{ε}, again taking as reference that $\Delta r_{\varepsilon} = 0$ for $\alpha = 1$. Fig.9 shows dependence of Δr_{ε} on Δr_{Ti}, which demonstrates that the radial shifts in Δr_{ε} and Δr_{Ti} are of comparable magnitude. For atoms of higher energies the influence is weaker since they come from deeper inside the plasma where the ion temperature is less affected by changing profile peakedness.

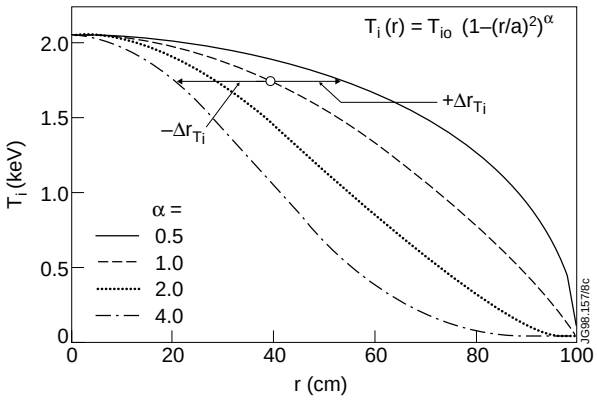

Fig.8: Hydrogen and deuterium ion temperature profiles with different peakedness α.

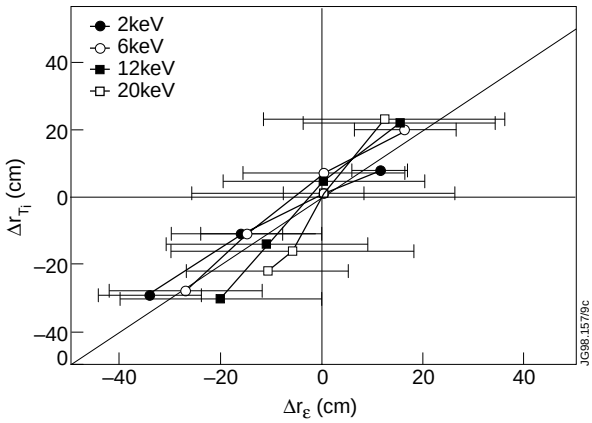

Fig.9: Movement in position of peak of emissivity function $\varepsilon(r,E)$ for atoms of different energies, as a function of corresponding movement in position of local ion temperature. Movement in positions of ε and local ion temperature are measured relative to the reference case with α=1.

3.4 Sensitivity of measured $R_{\Gamma}(E)$ to uncertainty in absolute ion temperature T_i.

We have investigated sensitivity of $R_{\Gamma}(E)$ to variation in absolute isotope ion temperature, keeping the isotope ion temperature ratio $R_T(r) = T_{D+}(r)/T_{H+}(r) = 1$, and the isotope density ratio $R_n(r) = 0.1 + 0.8\cdot(r/a)^2$. Recall that for $R_n(r)$= *constant*, variation in $R_{\Gamma}(E)$ will come about only due to unequal shift in the two emissivity profiles and unequal absorption, which is negligible. However, when $R_n(r)$ is not constant then different shifts in position of the two

emissivity profiles will take them into regions of different isotope ion densities which will in turn change $R_\Gamma(E)$ substantially. This was tested by varying the peak isotope ion temperature $T_i(0)$ with respect to its reference value T_{i0}, and simulating the measured isotope flux ratio. Fig.10 gives variation of isotope flux ratio with variation in peak isotope ion temperature, shown as $\left(R_\Gamma(T_i(0)) - R_\Gamma(T_{i0})\right) / R_\Gamma(T_{i0})$ Vs $\left(T_i(0) - T_{i0}\right) / T_{i0}$, for flux at different energies. The result is a consequence of two effects, a radial shift of the two emissivity profiles to regions of different isotope ion densities, and an exponential change in population of ions of pertinent energy due to Maxwellian energy distribution. The latter is illustrated by the behavior of fluxes at E=20 keV. Although the flux emanates from a region where $dR_n(r)/dr$ is small, the variation in ΔR_Γ is large due mainly to the Maxwellian ion energy distribution, as mentioned in section 3.2. Thus, uncertainty in absolute ion temperature causes uncertainty in $R_\Gamma(E)$, leading to an uncertainty in deduced shape and magnitude of $R_n(r)$.

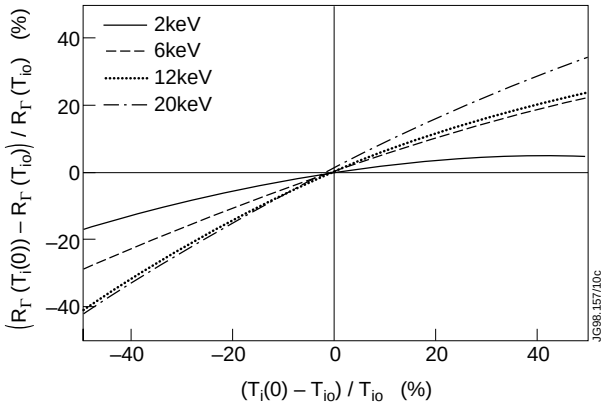

Fig.10: Dependence of flux ratio $R_\Gamma(E)$ on peak ion temperature $T_i(0)$, with $R_n(r) = 0.1 + 0.8 \cdot (r/a)^2$, $T_i(r)(eV) = T_i(0)\left(1 - (r/a)^2\right) + 10$, and $R_T(r) = T_{D+}(r)/T_{H+}(r) = 1$.

3.5 Sensitivity of measured $R_\Gamma(E)$ to uncertainty in temperature of ions and atoms at the plasma edge, $T_i(r = a)$ and $T_A(r = a)$.

To complete the investigation of sensitivity of measured flux ratio to uncertainty in plasma parameters we have simulated response of $R_\Gamma(E)$ to different edge ion temperature $T_i(a)$ and temperature of atoms entering the plasma $T_A(a)$. The effect of varying $T_i(a)$ is to shift radially the emissivity function, and that of varying $T_A(a)$ is to change the density of atoms in the plasma. No substantial effect of variations of $T_i(a)$ and $T_A(a)$ on $R_\Gamma(E)$ is observed. Fig.11 shows radial profile of $R_\Gamma(r)$ compared to profile of $R_n(r)$, for different $T_i(a)$. Fig.12 shows profile of $R_\Gamma(r)$ compared to that of $R_n(r)$, for different $T_A(a)$. Recall that the reference plasma has $T_i(a)$=50 eV, $T_A(a)$=10 eV. We see that $R_\Gamma(r)$ changes slightly with respect to $R_n(r)$, but the changes remain within the intrinsic uncertainty of $R_\Gamma(r)$.

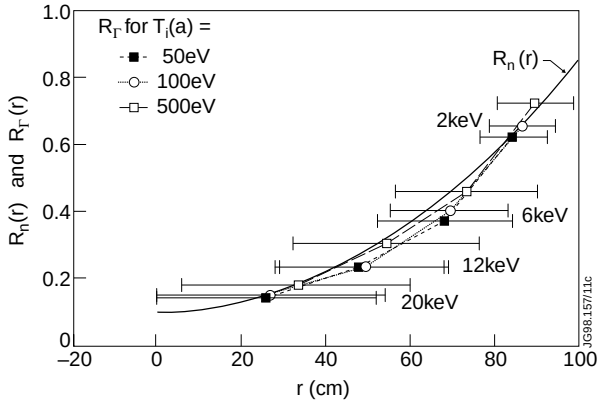

Fig.11: Radial dependence of $R_\Gamma(r)$, deduced from modeled flux ratio $R_\Gamma(E)$, compared to that of the density ratio $R_n(r)$, for different values of the edge ion temperature. We have assumed that $R_T(r) = T_{D+}(r) / T_{H+}(r) = 1$.

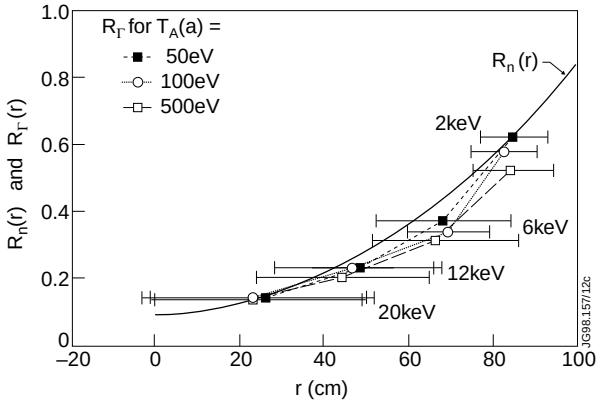

Fig.12: Radial dependence of $R_\Gamma(r)$, deduced from modeled flux ratio $R_\Gamma(E)$, compared to that of the density ratio $R_n(r)$, for different values of the edge atom temperature. We have assumed that $T_{D0}(a) / T_{H0}(a) = 1$.

4. DEDUCTION OF HYDROGEN ISOTOPE ION TRANSPORT BY MODULATION OF EDGE ISOTOPE ION DENSITY COMPOSITION.

Simultaneous measurements of atomic fluxes of different hydrogen isotopes from JET plasmas were routinely made using a time-of-flight NPA (KR2) [5,6]. The NPA was located at octant 3 with its horizontal line-of-sight along a torus major radius, and Z=0.28m above the torus mid-plane; the NPA line-of-sight thus intersected the plasma center. The experiments described in this section were performed with the intent to exercise the methodology of deducing the perturbed radial isotope ion density when the source was modulated. We also want to determine what the optimum conditions are for a good measurement of radial profile of isotope ion densities and transport. The experiment requires that the flux measurement be made with high time resolution while maintaining reasonable counting statistics. Limiting factors were overloading of start and stop detectors of the time-of-flight system by neutron and gamma-rays induced counts, and cross-talk between neighboring masses of atoms detected in the NPA channels. We therefore measured the fluxes with high time resolution, correcting for spurious counts due to random coincidences.

Deuterium gas injected into a hydrogen plasma with hydrogen NBI heating

Plasma pulses with NBI heating were selected because of the higher ion temperature and therefore larger flux in the high energy channels of the NPA. Short pulses of D_2 gas were injected to produce perturbation of the edge plasma ion density composition (pulses: 43397, 43413, 43414, 43421, 43446). Fig.13 shows evolution of the main plasma parameters for pulse #43446, which is typical for this series of pulses. The hydrogen plasma was fuelled mostly by recycling, and to a lesser extent by additional feed-back controlled hydrogen gas injection and all hydrogen NBI shown in fig.13. The NBI served also to heat the plasma. The hydrogen gas injection was applied at octant 3 at the mid-plane; this is close to the NPA and, by locally increasing the atom density

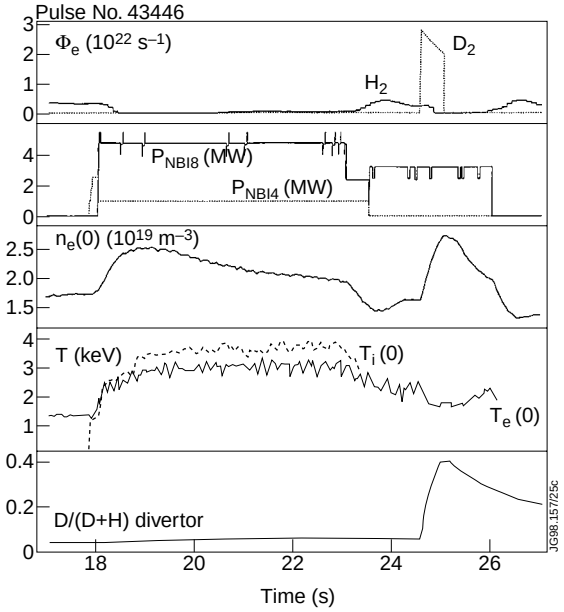

Fig.13: Evolution of main prameters of a hydrogen plasma heated by hydrogen NBI only. The top traces show the rate of hydrogen gas injection required to sustain the hydrogen plasma, and also deuterium gas pulse applied at 24.5s to perturb the edge deuteron density . The bottom trace shows the proportion of deuterium measured in the exhaust gases in the divertor.

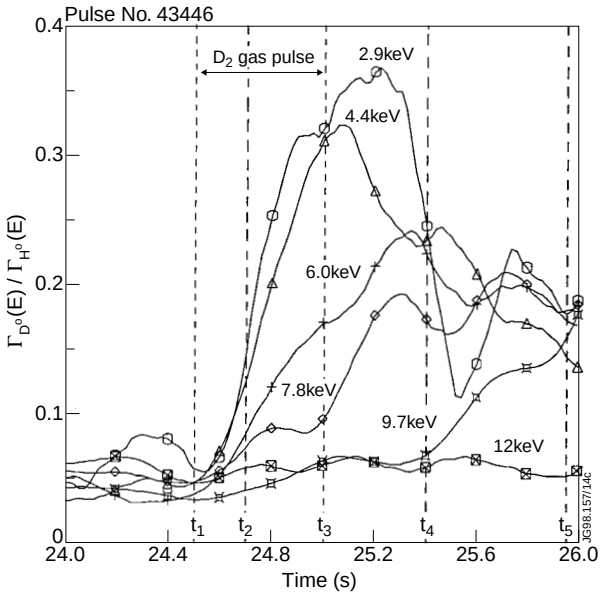

Fig.14: Evolution with time of the measured ratio $R_\Gamma(E)$ at different energies, for fluxes of deuterium and hydrogen atoms from plasma shown in fig.13. $R_\Gamma(E)$ at six energies, E(keV) = 2.9, 4.4, 6, 7.8, 9.7, and 12, and at five time points, $t_1 \rightarrow t_5$, was used for subsequent analysis.

in the plasma along the NPA line-of-sight, makes a good target for CX of plasma ions. A D_2 gas pulse was applied for 0.5s from t=24.5s at the mid-plane at octant 6, ≅ 9m toroidally from the NPA line-of-sight. The gas pulse was shorter in duration than the characteristic transport time of deuterons in the plasma, and the total number of ~1.2×10^{22} deuterium atoms were injected. Fig.14 shows the measured evolution of flux ratio $\Gamma_{D0}(E)/\Gamma_{H0}(E)$ for six energies spanning $2.9 \leq E(keV) \leq 12$, showing a tendency first to increase with time and then decrease and reach a new steady state. Unfortunately, for higher energies there is no clear evidence of increase or decrease of the flux ratio because first the H^0 flux to the NPA is dominated by CX of slowing-down of suprathermal hydrogen ions from the hydrogen NBI, and second the D^0 flux is strongly suppressed by cross-talk from the H^0 flux. Cross-talk between D^0 and H^0 in the NPA channels can be estimated in this case to be ≅5%. The remaining pulses in the series were performed with much larger H_2 gas pulses ($\cong 2 \cdot 10^{22}$ atoms/s for 4.6s, t = 18.2 - 22.8 s) during the oct.4 NBI. Perhaps for this reason the tendency of raising time with the energy is not observed for these discharges (see discussion below of the role of charge-exchange process in these measurements).

To deduce the radial profile of the isotope ion density ratio $n_{D^+}(r)/n_{H^+}(r)$ from energy dependence of flux ratio $\Gamma_{D0}(E)/\Gamma_{H0}(E)$ we simulated the atomic fluxes for the five time slices shown in fig.14. The following radial profiles of deuteron and proton density ratio $n_{D^+}(r)/n_{H^+}(r)$ gave the best fit to the measured flux ratio:

Time slice	time(s)	best radial profile of isotope ion density ratio
t1	24.5	$R_n(r) = n_{D+}(r)/n_{H+}(r) = 0.1$
t2	24.7	$R_n(r) = 5 - (5 - 0.1)[1 - (r/a)^{10}]$
t3	25.0	$R_n(r) = 13 - (13 - 0.1)[1 - (r/a)^{10}]$
t4	25.4	$R_n(r) = 2.8 - (2.8 - 0.1)[1 - (r/a)^{5}]$
t5	25.95	$R_n(r) = 1.2 - (1.2 - 0.1)[1 - (r/a)^{3}]$

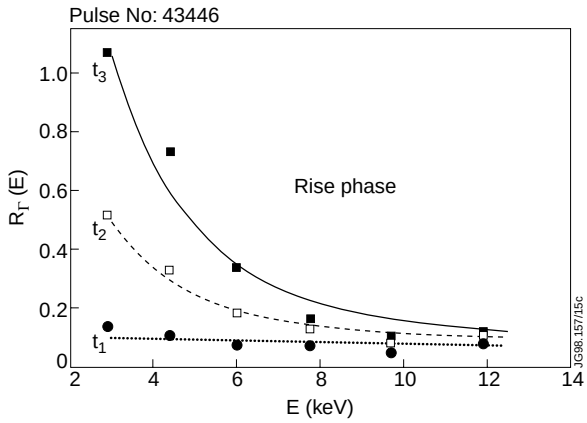

Fig.15: Measured and modeled $R_\Gamma(E)$ for time slices t_1, t_2, and t_3. The times correspond to the phase when $R_\Gamma(E)$ was observed to increase at all energies shown in fig.13, showing increasing deuteron density throughout the profile. Best fitting relative density $R_n(r) = n_{D+}(r)/n_{H+}(r)$ was determined; this is shown in section 4.1 in the main text.

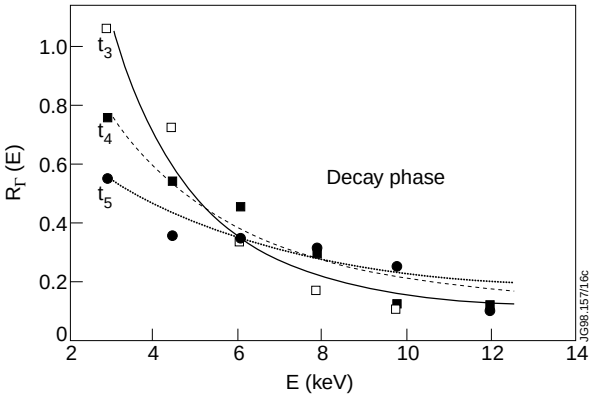

Fig.16: Measured and modeled $R_\Gamma(E)$ for time slices t_4, t_5, and t_6, during the decay phase of $R_\Gamma(E)$, showing deuteron density approaching a new equilibrium. Best fitting relative density $R_n(r) = n_{D+}(r)/n_{H+}(r)$ was determined; this is shown in section 4.1 in the main text.

Fig.15 and fig.16 show comparisons, respectively during rise and decay phases after injection of the D_2 gas pulse, of energy dependence of measured(points) normalized flux ratio $[\Gamma_{D0}(E)/\Gamma_{H0}(E)] \times [m_D/m_H]^{1/2}$ and simulation(curves) of the same quantity. In computing the curves in figs.15&16 we have used profiles of $R_n(r)$ given above. Fig.17 shows the best fitting $R_n(r)$ profiles tabulated above. In deducing $R_n(r)$ we have (a) ignored differences in temperature of the two ion species, (b) ignored uncertainty in absolute ion temperature or its radial profile, (c) assumed that $T_i(a)$=50 eV and $T_A(a)$=10 eV.

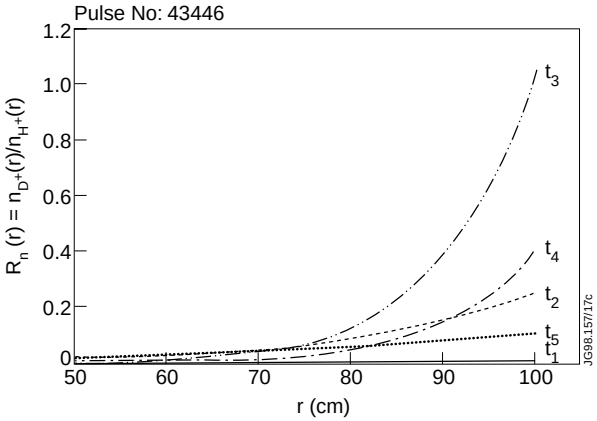

Fig.17: Best fitting relative density profiles $R_n(r) = n_{D+}(r)/n_{H+}(r)$ at different times, deduced from measurements shown in fig.14.

Finally we have deduced the evolution of radial profile of deuteron density, $n_{D+}(r)$, shown in fig.18, with $Z_{eff}(r)$ =1.3 and assuming that the underlying hydrogen ion density is unchanged. To deduce deuteron density transport into a hydrogen plasma we have assumed:

1. that the different isotope ions are transported independently in the plasma,
2. that atomic processes (charge-exchange, recombination, reionization etc) may be neglected, thus ignoring sources and sinks,
3. that the radial deuteron transport is diffusive, driven by the deuteron density gradient. The model for radial deuteron flux is $\Gamma_D(r,t) = -D(r,t) \times \nabla n_D(r,t)$. Moreover, in the following the possible variation of $D(r,t)$ is ignored, i.e. $D(r,t)$=constant = D_r.

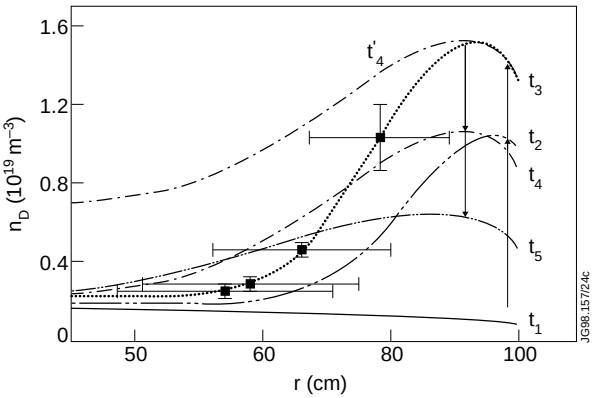

Fig.18: Evolution of deuteron density profile $n_{D+}(r,t)$ determined from data shown in figures 16&17, assuming that the radial profile of background hydrogen ion density did not change during this time.

For analysis of transport driven evolution of the deuteron density profile we have chosen the time interval $t_3 \rightarrow t_4$, where Δt = 0.4s, and spatial region from r = 70cm $\rightarrow$ 80cm. The reduction in deuteron density at the edge between t_3 and t_4 is due to reduction of deuterium injected at the edge. To take into account the reduction of deuterium flux between t_3 and t_4, the radial deuteron density profile at t_4 at r = 100cm was normalized to that at t_3 at the same position. The normalized profile is labeled t_4'. Assuming that evolution of the deuteron density at r < 100cm to be source-free, the diffusion equation is $\partial n_D / \partial t = -div\Gamma_D(r,t)$. In cylindrical geometry, with the flux model given earlier, the radial diffusion equation becomes

$$\frac{\partial n}{\partial t} = -D_r\left(\frac{\partial^2 n}{\partial r^2} + \frac{1}{r}\frac{\partial n}{\partial r}\right)$$

From the data shown in fig.18, we estimate that the magnitude of the different terms in the above equation is: $\partial n / \partial t = -9 \times 10^{12} cm^{-3} s^{-1}$, $1/r \times \partial n / \partial r = 8.5 \times 10^{9} cm^{-5}$, $\partial^2 n / \partial r^2 \approx 0$, giving $D_r \cong 1.1 \times 10^{3} cm^2 s^{-1}$. Therefore the time taken for a perturbation of deuteron density at the plasma edge to propagate to r = 75cm will be $\tau_{diff} \approx$ 0.57s, as observed. However, is the assumption of source-free evolution valid? Deuteron density at r = 75cm can increase because of transport from r > 75cm, or due to ionization of deuterium atoms at r = 75cm, by collisions with plasma electrons and ions. The ionization source of deuterons is $S = n_e n_{D0} < \sigma\upsilon >_i$. In the pulse analyzed, we have $n_{D0}(r = 75cm) = 5 \times 10^{6} cm^{-3}$, $n_e(r = 75cm) = 2.5 \times 10^{13} cm^{-3}$, and $< \sigma\upsilon >= 2 \times 10^{-8} cm^3 s^{-1}$, giving $S = 2.5 \times 10^{12} cm^{-3} s^{-1}$. Thus for pulse #43446 $\partial n / \partial t >> S$ and

the deuteron density evolution at r = 75cm is due to transport. However, in the other pulses of this series of experiments, the perturbing deuterium gas pulse was much bigger, as mentioned previously, so that $\partial n / \partial t \leq S$, precluding deduction of D_r.

The above example shows that the requirements of an optimum experiment to determine D_r are incompatible. In order to obtain a good measurement of the perturbed deuteron density the deuterium gas pulse needs to be strong. On the other hand a strong gas pulse produces too much deuterium atom density in the plasma and a source of deuterons which competes with and masks the deuteron transport, as shown above. It is difficult to predict by modeling what the best experimental procedure is to deduce D_r. We will attempt to answer these questions empirically at the next opportunity. Strong gas injection in the divertor, and NBI from octant 8 are two of the tools that might also be used for this purpose.

5. SUMMARY.

1. Simulations of formation of efflux of hydrogen isotope atoms show that energy dependence of ratio of fluxes can be successfully used to deduce the corresponding radial ion density profiles with the spatial accuracy $\Delta r/a \approx 30$ - 45 % in the region $0.3 \leq r/a \leq 0.9$. Accurate hydrogen isotope ion temperature profile is a key requirement of the measurements. Uncertainties in absolute ion temperature and profile peakedness cause large uncertainties in deduced radial profile $R_n(r) = n_{D+}(r) / n_{H+}(r)$.
2. Analysis of an experiment in which D_2 gas pulse was injected into a hydrogen plasma heated by hydrogen NBI was done to deduce evolution of the perturbed deuteron density profile. Radial deuteron density diffusivity $D_r \cong 1.1 \times 10^3 cm^2 s^{-1}$ was deduced for $70 \leq r(cm) \leq 80$. This determination is very crude at present.
3. From the modeling of formation of effluxes of hydrogen isotope atoms, and analysis of the experiments to determine the perturbed deuteron density profile, we learn that optimum conditions for realizing the intended program are:
   (a) measurements in plasmas with high ion temperatures, achieved with NBI and ICRH.
   (b) the gas pulse used to perturb the minority isotope species should be applied in the divertor plasma.
   (c) low recycling conditions are best, because then large injection of gas is required to maintain the majority isotope ion density. This should be done in front of the NPA line-of-sight at octant 3 midplane, thus producing a good atomic density profile and strong charge-exchange flux of atoms to the NPA.

6. REFERENCES

[1] Yu.N.Dnestrovskij, S.E.Lysenko, and A.I.Kislyakov, Nuclear Fusion, **19**(1979)293.

[2] Yu.N.Dnestrovskii and D.P.Kostomarov, Section 4.2.4 in *Numerical Simulation of Plasmas*, Springer-Verlag, Berlin, 1986.

[3] Yu.S.Gordeev, A.N.Zinov'ev, and M.P.Petrov, JETP Letters, **25**(1977)204.

[4] A.B.Izvozchikov, Dissertation for degree of *Candidate of Science*, A.F.Ioffe Physico-Technical Institute, St. Petersburg, 1980.

[5] G.Bracco and K.Guenther, *JET Report* JET-R(96)041

[6] K.Guenther, Preliminary study of the T/(T+D) mixture ratio in some selected discharges, unpublished.